https://doi.org/10.5194/amt-2023-193
Preprint. Discussion started: 20 September 2023

Atmospheric Measurement Techniques Discussions

A Modified Gaussian Plume Model for Mobile in situ Greenhouse Gas Measurements

Lawson D. Gillespie[1,2], Sébastien Ars[2], James P. Williams[3], Louise Klotz[3], Tianjie Feng[1], Stephanie Gu[1], Mishaal Kandapath[1], Amy Mann[1], Michael Raczkowski[1], Mary Kang[3], Felix Vogel[2], and Debra Wunch[1]

[1]Department of Physics, University of Toronto, Toronto, ON, Canada
[2]Climate Chemistry Measurements and Research, Climate Research Division, Environment and Climate Change Canada, Toronto, ON, Canada
[3]Department of Civil Engineering, McGill University, Montréal, QC, Canada

Correspondence: Lawson Gillespie (lgillespie@physics.utoronto.ca)

Abstract.

Atmospheric methane measurements are important for evaluating high resolution methane inventories and monitoring emissions reductions. Despite recent international efforts to harmonize measurement methodologies and techniques, currently there are no standardized or internationally accepted techniques for estimating emissions from mobile in situ concentration measurements. We present measurements from two different mobile in situ methane laboratories, and compare emission rates calculated from four Gaussian plume Bayesian optimal estimation strategies and a statistical algorithm. For mobile transects from the slower flow-rate instrument, we find a significant asymmetric smoothing artifact. The effect of this asymmetry is most significant for short transects of small (0-50 kg CH_4 day^{-1}), nearby methane sources, where the plume crossing time is comparable to the mean residence time of the instrument. We develop a model of this effect, demonstrate how this model can be applied to Gaussian plume inversions, and describe its limitations. We use these results to compute emissions rate estimates for two methane sources from Toronto's wastewater management system to demonstrate the use and limitations of Gaussian plume inversions to quantify methane emissions in an urban environment. Overall, we highlight the importance of using observed plume enhancement areas rather than the more commonly used enhancement heights for determining comparable emissions estimates between different mobile laboratories.

1 Introduction

Mitigating anthropogenic methane emissions is one of many critical steps necessary to combat climate change. Atmospheric measurements are necessary to monitor and validate the impact of the emissions reductions strategies taken by municipal, regional, and national entities in order for us to track our progression towards new climate targets. Cities have been at the forefront of planning necessary decarbonization pathways, including Toronto's TransformTO aim to achieve net zero CO_{2eq} emissions by 2040 (The City of Toronto, 2021). Methane has a global warming potential that is 28 times that of CO_2 over a 100 year period, and is a valuable energy resource (IPCC, 2013). In the atmospheric carbon cycle, methane eventually reacts to form CO_2, so mitigating emissions by flaring, or fuel use is less harmful than allowing direct emissions of methane to the

https://doi.org/10.5194/amt-2023-193
Preprint. Discussion started: 20 September 2023


Atmospheric Measurement Techniques Discussions

atmosphere (Kirschbaum, 2014; Tavakkoli et al., 2022). In the urban environment, when compared to the nearly-ubiquitous emissions of CO_2, there is a relatively small number of highly emitting facilities and point sources of CH_4, making it a good candidate for mobile survey measurement strategies. There are two significant sources of methane emissions from methane gas fuel use in urban environments. To distinguish emissions from the primarily fossil fuel derived gas used for domestic energy use from the biogas produced at sanitation facilities, we will use the terms fossil gas, and biogas, respectively. In the EDGARv7.0 greenhouse gas emission inventory, cities account for approximately 15% of anthropogenic methane emissions in Canada (Crippa, M. et al., 2022). For the Greater Toronto Area, Canada's largest and most populous metropolitan area, the Facility Level and Area Methane Emissions (FLAME-GTA) inventory is the most detailed and comprehensive assessment of methane emissions (Pak et al., 2021). FLAME-GTA, as with other emissions inventories, relies on bottom-up accounting methods, generally either derived from emissions factors weighted by population density, or production activity. Uncertainties in these emissions factors can be significant; in some cases larger than 50%. Additionally, bottom-up inventories are not exhaustive lists, potentially missing emissions sources, particularly smaller industrial sources which are below reporting thresholds and small point sources from sewers or pneumatic valves in the fossil gas distribution system (Williams et al., 2022). Mobile emissions monitoring using atmospheric in situ measurements is a useful technique for verifying emissions and constraining inventory uncertainties for point sources and facilities, and tracking the seasonal trends of those methane emissions. However, mobile in situ monitoring is not able to easily quantify diffuse emissions sources, such as urban wetlands, post-meter indoor gas leaks, and inefficient appliance combustion, which have recently been shown to be a significant contributor to the urban atmospheric methane burden (Lebel et al., 2022; Herrero Ortega et al., 2019).

There is a large and growing body of literature utilizing vehicle based mobile in situ GHG concentration data to estimate methane emissions from known sources using a variety of techniques. Currently, research groups utilize different gas analyzers, experimental setups, and data analysis techniques for estimating methane emissions from mobile in situ data. In order for this data to be useful for inventory assessment purposes and comparable to other studies, standardized or comparable measurement methodologies should be adopted. Recently, there has been an effort to harmonize methodologies used to quantify emissions from mobile in situ measurements to improve the comparability of estimates from different researchers and organizations (Turnbull et al., 2022; Wielgosz et al., 2023).

Here, we present a brief summary of common methodologies used to analyze mobile in situ CH_4 concentrations. The first such technique is the coincidental controlled release, where a gas is released into the atmosphere with a known emission rate near a GHG emission source with an unknown emission rate. Both gases are measured simultaneously during a mobile survey, allowing for a simple tracer ratio calculation to estimate emissions. This technique has been used to measure emissions from urban infrastructure (Lamb et al., 1995; Shorter et al., 1996), landfills (Mønster et al., 2015), and fossil oil and gas infrastructure (Lamb et al., 2015; Delre et al., 2022).

It is not always practical or possible to conduct coincidental controlled release experiments, as additional instrumentation or site access is often required. When coincidental controlled release experiments are not possible, Gaussian plume inversions of a single measured gas have been used to quantify methane emissions from a variety of different sources, including emissions from the oil and gas sector in Canada (Atherton et al., 2017; Zavala-Araiza et al., 2018; Baillie et al., 2019; O'Connell et al.,

https://doi.org/10.5194/amt-2023-193
Preprint. Discussion started: 20 September 2023

Atmospheric Measurement Techniques Discussions

2019; Vogt et al., 2022), the United States (Yacovitch et al., 2015), and Europe (Yacovitch et al., 2018; Kumar et al., 2022). One study in the United States utilized this technique for quantifying emissions from 63 wastewater treatment plants (WWTP) (Moore et al., 2023). Other mobile experiments have utilized multiple GHG analyzers measuring at different inlet heights, which allows for a more thorough analysis of observed downwind plumes, which has been used to quantify CH_4 emissions from active and inactive oil and gas infrastructure (Rella et al., 2015; Lebel et al., 2020). A third prominent technique utilizing mobile platforms for quantifying emission rates from in situ measurements is the Other Test Method (OTM) 33a technique, which estimates emissions from the co-variation in downwind concentration and wind direction for a stationary downwind sensor (Thoma and DeWees, 2014). Mobile measurement platforms are typically parked downwind of sources for 20-30 minute periods to determine how concentrations vary with wind direction. This technique has been used to measure CH_4 emissions from oil and gas infrastructure in the United States (Brantley et al., 2014), Canada (Vogt et al., 2022; Hugenholtz et al., 2021), Europe (Yacovitch et al., 2018; Kumar et al., 2022), and compressed fossil gas facilities in Eastern China (Wang et al., 2022). Collectively, these in situ emissions quantification techniques have enabled researchers to quantify emissions from individual facilities, in addition to updating national inventory estimates on a sector-wide basis (MacKay et al., 2021).

Quantifying emissions from urban sources can be challenging because individual point sources of methane emissions can be harder to correctly identify in an environment with more built infrastructure, wind tunnelling, and gas distribution leakage. However, Gaussian plume inversions of mobile in situ data have been used to quantify urban methane emissions from known sources using vehicle based surveys (Ars et al., 2020; Maazallahi et al., 2020; Moore et al., 2023) and walking surveys (Chen et al., 2020). One study used a computational fluid dynamics model to drive a large eddy simulation to invert observed mobile in situ CH_4 plumes from large sources in Indianapolis (Lamb et al., 2016).

In addition to the aforementioned quantification strategies, which explicitly account for the location and likely source of emissions, statistical algorithms have been developed to estimate emissions rates from leaks in fossil gas distribution based solely on observed atmospheric concentration enhancements measured by mobile in situ laboratories (Von Fischer et al., 2017; Weller et al., 2019). These algorithms are most useful for datasets missing the required meteorological or source location data necessary for specific plume attribution and quantification. They have been widely applied to urban survey data for determining relevant statistics on the size and variability of fugitive methane emissions from urban fossil gas distribution networks (Weller et al., 2020; Ars et al., 2020; Defratyka et al., 2021; Maazallahi et al., 2020; Fernandez et al., 2022; Vogel et al., 2023a).

All of these emissions quantification strategies can be evaluated using controlled release experiments, where the target gas of interest is released into the atmosphere at a known rate. Such experiments have been widely used to evaluate and calibrate different emissions quantification methodologies (Von Fischer et al., 2017; Ars et al., 2017; O'Connell et al., 2019).

In this paper, we analyze a dataset consisting of mobile in situ atmospheric methane concentrations collected in the Greater Toronto Area. We evaluate various Gaussian plume inversion strategies, and other emissions quantification methodologies using data from a controlled release experiment and from surveys downwind of two types of wastewater facilities. In Section 2, we describe the datasets and inversion strategies. We evaluate the impact of different GHG analyzers with different flow rates on our observed mobile transect data, and in Section 2.3, we develop an instrument response function for the instrument with the slower flow-rate. In Section 2.4, we analyze data from a controlled release experiment to evaluate the inversions. In

https://doi.org/10.5194/amt-2023-193
Preprint. Discussion started: 20 September 2023


Atmospheric Measurement Techniques Discussions

Section 3, we apply our Gaussian plume inversion methods to quantify emissions from urban wastewater infrastructure. In Section 4, we compare and discuss the emission rate quantification techniques. Finally, in Section 5, we present conclusions and implications for future mobile GHG quantification experiments.

2 Methods

In this section, we describe the datasets collected using our mobile laboratories in Section 2.1, and our Gaussian plume inversion techniques in Section 2.2. We describe the need for developing an instrument response function for our slower flow-rate instrument in Section 2.3, and evaluate the inversion techniques with and without the instrument response function among other sensitivity studies in Section 2.4.

2.1 Datasets

Since 2017, we have used a Los Gatos Research (San Jose, CA) Ultraportable Greenhouse Gas Analyzer (UGGA) to measure atmospheric concentrations of CO_2, CH_4, and H_2O from a mobile bicycle-trailer-based laboratory around the City of Toronto, Ontario, Canada (Figure 1a). Simultaneous 1 Hz GHG concentrations, meteorological information, and GPS position data are logged on a laptop computer. We have also occasionally used this analyzer in a vehicle based laboratory to survey sites outside of the city, but these data are not evaluated in this work, aside from a side-by-side comparison described in the Supplemental Information (S1.1). Since 2018, we have also used a vehicle based mobile laboratory which is equipped with various Picarro cavity ring-down spectrometers (G1301, G2401) fitted with exterior high flow-rate pumps to record CH_4, CO_2 and H_2O concentrations every two seconds (Figure 1b). Both platforms are described further in Ars et al. (2020), and in the Supplemental Information (S2). In this paper, our focus is on the methane and meteorological measurements from both mobile laboratories (Wunch et al., 2018; Ars et al., 2019; Gillespie et al., 2022a, b, 2023).

2.2 Gaussian Plume Inversions

We estimate instantaneous CH_4 emissions rates by using Bayesian optimal estimation to fit a Gaussian plume dispersion model to our downwind concentration enhancement measurements. In order to estimate an instantaneous emission rate from an emission source, such as a WWTP or power plant, we use the mobile laboratories to transect plumes downwind of methane sources. To isolate the contribution of specific sources, we subtract the fifth percentile concentration to remove the local background concentration, isolating the concentration enhancements from the upwind source. Then, we use these concentration enhancements to model the upwind emission rates.

When optimizing the Gaussian plume model, one must choose which scaling factor to optimize. Two common choices to scale are the enhancement height or the enhancement area. These scaling factors comprise a vector of scaling factors, $\boldsymbol{p}$, with each element of the vector describing an equal distance portion of the transect to be optimized. The enhancement height is the difference between the maximum concentration in the plume and the background concentration. The enhancement area is the integral of the plume enhancement above the background. Both of these quantities are sketched in Figure 2. The plume vector

https://doi.org/10.5194/amt-2023-193
Preprint. Discussion started: 20 September 2023

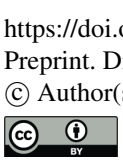

Atmospheric Measurement Techniques Discussions

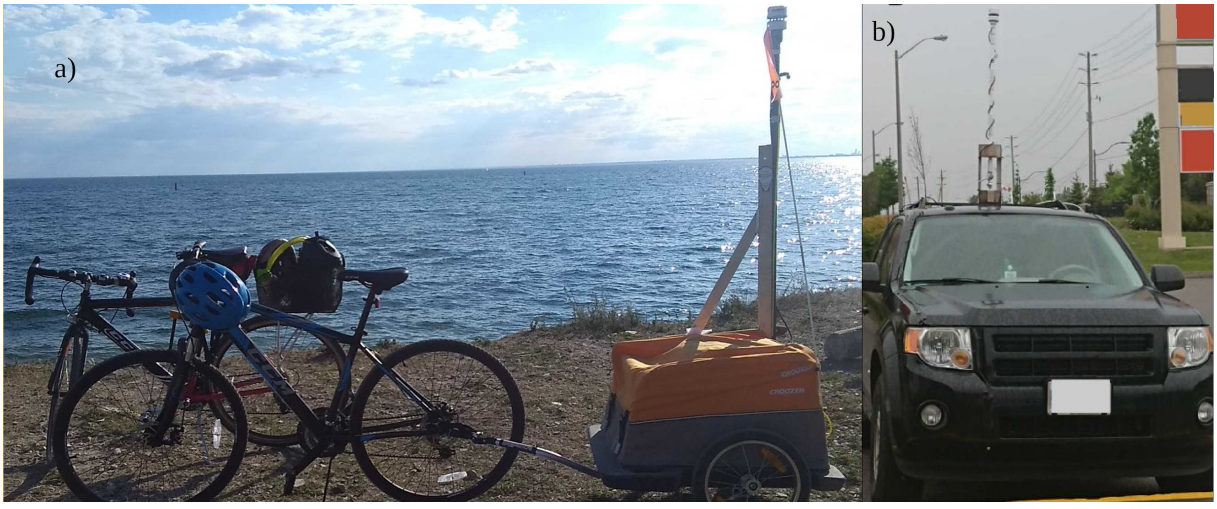

Figure 1. (a) The University of Toronto's bicycle based laboratory equipped with an LGR UGGA. (b) ECCC's vehicle based laboratory equipped with a Picarro G1301 or G2401. Both setups use Airmar WX220 weather stations to record meteorological and GPS data.

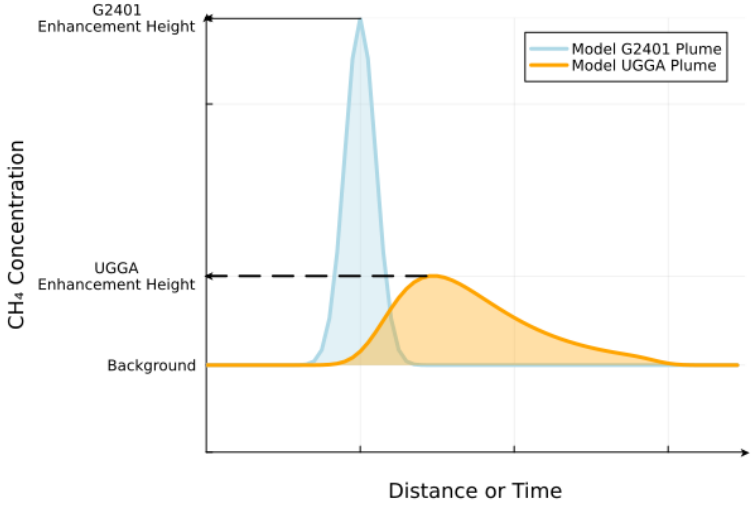

Figure 2. A model representation of the trace gas concentrations in narrow downwind plumes as observed by our mobile laboratories for an identical emission event. The shaded plume areas are the same, while the enhancement height for the UGGA is significantly lower.

is related to the Gaussian dispersion model:

$$\boldsymbol{p} = \mathbf{H}\boldsymbol{f} + \epsilon_0 \tag{1}$$

where ϵ_0 represents the combined uncertainties resulting from measurement uncertainty in the methane concentrations, and uncertainties from the determination in the background concentration. $\mathbf{H}$ is the operator that transforms the vector of emission rates, $\boldsymbol{f}$, which are in units of mass·time^{-1}, into the plume vector, $\boldsymbol{p}$ space, which is in units of ppb, ppb·m, or ppb·s. There

https://doi.org/10.5194/amt-2023-193
Preprint. Discussion started: 20 September 2023


Atmospheric Measurement Techniques Discussions

are two options for the plume axis when optimizing the enhancement area: one can integrate under the enhancement curve using units of time (ppb·s) or distance (ppb·m). When the mobile laboratory maintains a steady velocity during the transect, there is little difference between these methods. However, if the mobile laboratory stops during the transect, then a time-based inversion would weigh each observation equally in time, while the distance-based model would correctly weigh the data point from the stationary location. If a significant portion of the plume transect is spent in stop-and-go traffic, an inversion optimizing the concentration-time area might be preferential to take into account more of the observed data.

The Bayesian optimal estimate of the emissions, $\boldsymbol{f^a}$, can be calculated as

$$\boldsymbol{f}^a = \boldsymbol{f}^b + \mathbf{B}\mathbf{H}^T \left(\mathbf{R} + \mathbf{H}\mathbf{B}\mathbf{H}^T\right)^{-1} \left(\boldsymbol{p} - \mathbf{H}\boldsymbol{f}^b\right), \tag{2}$$

where $\boldsymbol{f}^b$ is the vector of prior emissions rates, $\mathbf{B}$ is a matrix representing the uncertainty in the prior emissions estimate. For all of our inversions, we assume an 80% uncertainty in our prior values, so that our inversions are only loosely constrained by our priors. $\mathbf{R}$ is a matrix representing the atmospheric transport model errors, and other measurement errors from the background determination and instrumentation errors. In our inversion, we assume that $\mathbf{B}$ and $\mathbf{R}$ are diagonal matrices. We assume constant values for $\mathbf{R}$, depending on the transect distance. For our small plumes, we use a value of 1500 ppb·m, and for the larger transects, we used a model error of 15 000 ppb·m. The variance-covariance uncertainty matrix, $\mathbf{A}$, is defined as

$$\mathbf{A} = \left(\mathbf{B}^{-1} + \mathbf{H}^T\mathbf{R}^{-1}\mathbf{H}\right)^{-1}. \tag{3}$$

Information in the $\mathbf{A}$ matrix can also be used to determine how well each source in the optimal estimate vector, $\boldsymbol{f}^a$, is constrained by the inversion, as well as to provide an estimate of the uncertainty of the inversion.

The Gaussian plume dispersion model we use is the Polyphemus air quality modelling system (Mallet et al., 2007). The horizontal and vertical diffusivities in Polyphemus are the Brigg's formulation of the Pasquill-Turner stability classes, which is a flexible parameterization of the Gaussian plume model (Briggs, 1973). The stability classes are determined from the insolation, surface wind speed, and surface roughness estimated from land cover type. When reliable stationary in situ meteorology data are available, we use the σ_a method of determining transect-specific stability classes, which uses wind speed and variability in azimuthal wind direction to determine stability class (Bailey et al., 2000). We adjust the initial model parameters, principally wind direction, to align observed and modelled Gaussian plumes. Then, we use this wind-rotated Gaussian plume dispersion model as our operator, $\mathbf{H}$.

2.3 Instrument Response Function

For many of our small plume transects observed with the bicycle laboratory, the standard Gaussian plume model provides a poor fit to our observations. Similar to the findings of Takriti et al. (2021), we observe a significant smoothing of the measured plumes, which is a consequence of the lower flow-rate of air through the instrument relative to the plume transect time. The low flow-rate of the UGGA causes an asymmetric smoothing for short plume transects where the time it takes to cross the plume is similar to the mean residence time of the instrument. The UGGA's mean residence time in the detection cavity is around 8 seconds with our setup. This, combined with the 1Hz sampling frequency resolves the asymmetric instrument

https://doi.org/10.5194/amt-2023-193
Preprint. Discussion started: 20 September 2023

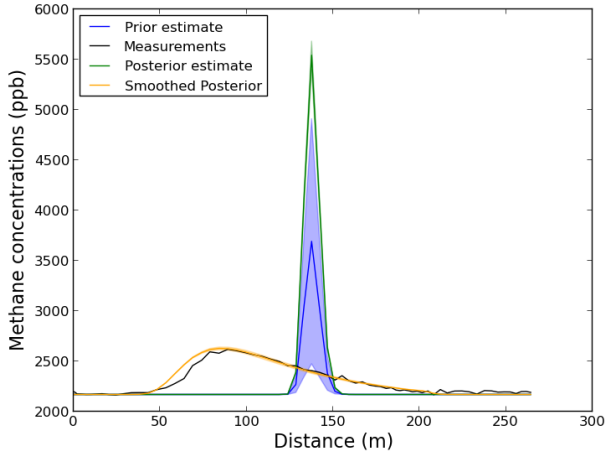

(a) The methane concentrations observed during the third UGGA transect of the 9.45 kg per day release.

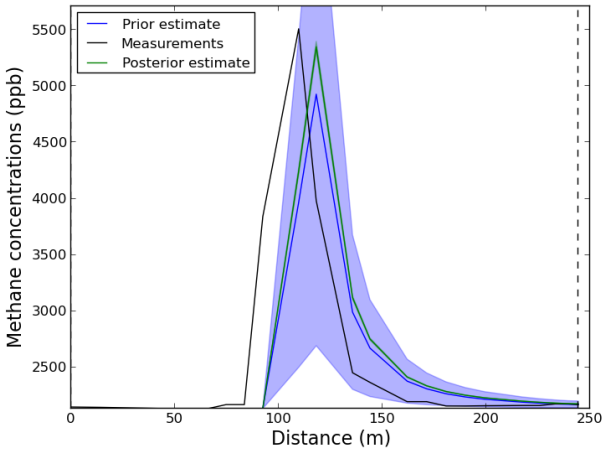

(b) The methane concentrations observed during the first G2401 transect of the 18.8 kg per day release.

Figure 3. Examples of measurements collected by the mobile platforms downwind of the gas outlet during the controlled release experiment. In panel (a), one transect from LGR UGGA measurements is shown from the 9.45 kg·day^{-1} release. In panel (b), a Picarro G2401 measurement transect is shown from the 18.8 kg·day^{-1} release. The measured CH_4 concentrations are shown in black and plotted as a function of the transect distance in metres. The Gaussian plume prior concentrations are shown in blue, and the Gaussian plume posterior is green. The posterior of the smoothed Gaussian plume area inversion is shown in orange in panel (a).

response function when sampling a narrow concentration perturbation. For the Picarro instrument in vehicle based lab, the mean residence time is roughly half of the sampling frequency, 0.5Hz. This, when combined with the slower sampling frequency, means that observations better represent in situ concentrations in space, which agrees better with the Gaussian plume models. A model representation of the concentrations measured by the two instruments for a transect that lasts on the order of 8 seconds is shown in Figure 2. A similar figure showing real data is in Figure S1.

To more accurately model the instrument response function, we use a normalized heavy-tailed distribution function given by equation 4.

$$f(t,\sigma,\mu,n) = \frac{\frac{1}{\sigma\sqrt{2\pi}} \exp \frac{-(\log t-\mu)^2}{2\mu^2}}{\sum_0^n \frac{1}{\sigma\sqrt{2\pi}} \exp \frac{-(\log t-\mu)^2}{2\mu^2}}, \tag{4}$$

where t is the measurement time in seconds, μ is a variable adjusting the horizontal coordinate of the vertex, σ is a variable adjusting the vertical coordinate of the vertex, and n is the length of the convolution window. The values of the variables chosen to represent the instrument response function for the UGGA are n = 37, μ = 2.2, and σ = 0.65. These values were estimated by fitting our observed concentrations to Gaussian plume models, and from a vehicle based campaign where coincident measurements from the higher flow-rate Picarro G2401 and LGR UGGA were conducted. Convolving the observed Picarro measurements with our asymmetric smoothing function (Equation 4) significantly increases the correlation between the mobile

https://doi.org/10.5194/amt-2023-193
Preprint. Discussion started: 20 September 2023

Atmospheric Measurement Techniques Discussions

Table 1. Summary of main results from the controlled release experiment using the σ_a method for prescribing P-G Stability Classes

Methane Release Rate ($kg \cdot day^{-1}$)	Number of Bicycle Transects	Number of Car Transects	Mean Estimated Emission Rate ($kg \cdot day^{-1}$) [Bike, Enhancement Area]	Mean Estimated Emission Rate ($kg \cdot day^{-1}$) [Car, Enhancement Area]
2.36	3	7	1.7 ± 0.5	2.9 ± 1.8
4.72	3	4	6.7 ± 0.6	8.1 ± 8.0
9.45	2	3	15.6 ± 0.6	11.7 ± 12.7
18.89	4	5	22.2 ± 19.7	17.4 ± 4.8

observations (Figure S1). Further discussion of this experiment is found in the Supplemental Information (S1.1). An example of a smoothed Gaussian plume model, compared to measured concentrations is also shown in Figure 3 a.

We evaluate four different versions of the Gaussian plume inversion using a controlled release experiment described in Section 2.4. The four versions are: 1. enhancement height, 2. enhancement area, 3. smoothed enhancement height, and 4. smoothed enhancement area. Tests 3 and 4 apply smoothing by convolving the modelled concentrations with the instrument response function in Equation 4.

2.4 Controlled Release Experiment

On 20 October 2021, we released CH_4 at a controlled and known emission rate, using a Masterflex proportional flowmeter controller. For the duration of the experiment, the gas outlet was located at ground level on the sidewalk in Toronto's industrial Port Lands neighbourhood, at the coordinates ($43.655008°$N, $-79.325247°$W), as shown in Fig S2. There were no buildings between the release location and the downwind transects, which were conducted in a live traffic environment. Wind speed and direction were recorded at the release location with a Vaisala WXT536 weather station at a 2m height directly above the gas outlet for the duration of the experiment. Wind roses from the release period from the three wind sensors, the stationary Vaisala WXT536, and two mobile Airmar WX220 units are discussed in the Supplemental Information (S3.3), but winds were most often from the WSW with a 75th percentile wind speed of 2.0 ms^{-1}. Both the bicycle laboratory and vehicle based setup measured multiple transects of each of the four release rates, summarized in Table 1.

We designed this experiment to simulate small urban plume conditions often encountered in our bicycle and vehicle surveys. These plumes are often transected very near the emissions sources. Transect inversions at these distances are highly uncertain, as the horizontal and vertical plume dispersion is generally not well mixed at these distances. Additionally, the uncertainty in emission rate estimates is expected to asymptote as the distance from the source approaches zero (Ars et al., 2017). After we noticed a significant variability in inversion results from the bicycle laboratory's closest transects, we removed transects with a minimum distance to the emissions source of less than 6.25m. Results using closer transects are discussed further in the Supplemental Information (S3.4). Comparing the observations between the ECCC vehicle laboratory and the UofT bicycle lab, the asymmetric smoothing is obvious in the UGGA plumes, and is less evident in the plumes observed with the faster flow-rate

https://doi.org/10.5194/amt-2023-193
Preprint. Discussion started: 20 September 2023

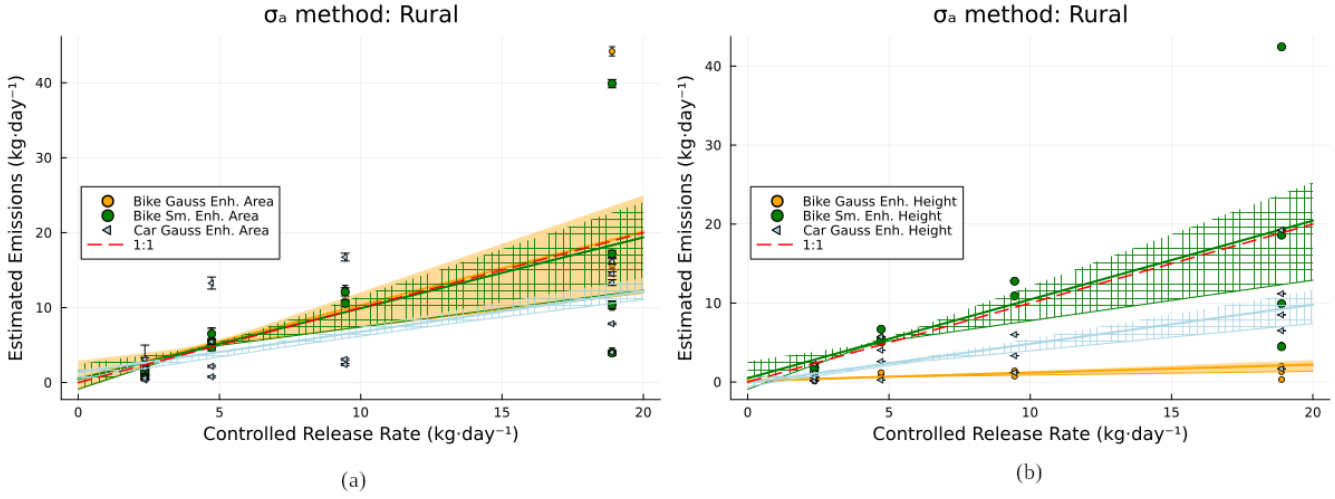

Figure 4. The estimated CH_4 emission rates are plotted against the known emission rate from our controlled release experiment performed on 2021-10-20. (a) shows estimates calculated using the enhancement area calculations, and (b) shows the emissions estimates calculated using the enhancement heights. Data from the UGGA bicycle lab estimates calculated using the normal Gaussian plume inversions are shown in orange. The green shows the estimates from the same bike data calculated using the smoothed Gaussian plume inversions. The Gaussian plume estimates from the G2401 vehicle are shown in light blue. The ribbons indicate the total range of bootstrapped linear fits to these data.

Picarro setup, as seen in two plumes in Figure 3. A summary of the estimated emissions rates using the enhancement areas, and enhancement heights for the vehicle as well as the smoothed Gaussian enhancement area and height for the bicycle laboratory are shown in Figure 4.

From our controlled release experiment, we compute a linear regression between the emissions estimates from the bicycle based lab and the known release rate. Using the σ_a method of azimuthal wind fluctuations for determining P-G stability class (Bailey et al., 2000; Mitchell, 1982), the slope and uncertainty of the fit is 1.18 ± 0.46. For the vehicle laboratory, the slope of the line of best fit is 0.83 ± 0.21. This demonstrates that for these nearby, close-to-source transects, we can assume a nominal uncertainty on the order of 40% for inversions measured with the bicycle lab.

The largest source of uncertainty in Gaussian plume inversions is typically from the choice of atmospheric stability class (Ars et al., 2017), and therefore similar plots for each stability class are shown in Figure S3. Table 2 gives the slopes of the lines of best fit for the controlled release experiments evaluated with different stability classes calculated using the Gaussian enhancement area for the bicycle lab, the vehicle lab, and the combined datasets.

For the UGGA bicycle lab, results comparing the Gaussian height inversions and the smoothed height inversions are presented in Figure S4, and Figure S5 shows the UGGA smoothed height inversions alongside the car's Gaussian plume height inversions. Generally, the Gaussian height inversions for the UGGA systematically return smaller optimized emission rates. The smoothed enhancement height inversions for the UGGA lab are consistent with the area-based inversions, demonstrating that one must account for the instrument response function of the UGGA only when optimizing the enhancement height of the

https://doi.org/10.5194/amt-2023-193
Preprint. Discussion started: 20 September 2023

Atmospheric Measurement Techniques Discussions

Table 2. Summary of the slopes for the best fit lines estimated with transects from our controlled release experiments using different stability classes and the Gaussian enhancement area.

Stability Class	Bicycle Data Line of Best Fit	Car Data Line of Best Fit	Combined Data Line of Best Fit
Rural A	1.66 ± 0.67	1.18 ± 0.24	1.39 ± 0.29
Rural B	1.20 ± 0.46	0.83 ± 0.21	0.98 ± 0.21
Rural C	1.14 ± 0.42	0.75 ± 0.33	0.91 ± 0.25
Urban A/B	1.96 ± 0.80	1.50 ± 0.27	1.71 ± 0.34
Urban C	1.66 ± 0.67	1.18 ± 0.24	1.39 ± 0.29
Rural σ_a	1.18 ± 0.46	0.83 ± 0.21	0.98 ± 0.22
Urban σ_a	1.94 ± 0.80	1.19 ± 0.25	1.52 ± 0.34

Gaussian plume model. The Gaussian enhancement height inversions for the Picarro also underestimate the emissions with respect to the enhancement area inversions with a best fit slope of 0.65 ± 0.16. The UGGA is significantly more underestimated, with a best fit slope of 0.12 ± 0.05.

The smoothed plume enhancement height inversions were affected more severely by outliers, and have a slope and offset further from the 1:1 line than the area inversions.

Based on the results of our controlled release experiment, we argue that when optimizing emissions using the emissions enhancement height, it is necessary to account for the instrument flow-rate, particularly for low flow-rate instruments. We find that simply using the Gaussian plume area, whether or not we take into account the instrumental smoothing, also provides a better estimate of the release rate. Accounting for smoothing in enhancement area inversions does not significantly change the results. These findings agree well with previous studies by Ars et al. (2017), Ars et al. (2020), and Takriti et al. (2021). As a practical application of our insights in inversion comparability, for the remainder of this paper we present emissions derived using the plume area. Further discussion of the different emissions quantification techniques is found in Section 4.

3 Quantifying Methane Sources in the Greater Toronto Area

In this section, we quantify emissions from plume transects downwind of large and small methane emissions sources, demonstrating the importance of accounting for the instrument flow-rate for modelling our shorter, near-to-source transects. In Section 3.1, we present the Gaussian plume inversion results for downwind transects of the largest wastewater treatment facility in the Greater Toronto Area, the Ashbridge's Bay Wastewater Treatment Plant (ABWWTP). These plume crossings are, at the closest, 100 m from the modelled sources, and a short plume transect of this facility is nearly 1 km long, which takes between 3-10 minutes to transect by bicycle. Under these conditions, smoothing the Gaussian plume model has minimal impact for modelling our mobile in situ CH_4 observations. In Section 3.2, we present our results from observed methane plumes from the storage shafts of the Western Beaches Tunnel system, a series of three underground storage basins for retaining Combined

https://doi.org/10.5194/amt-2023-193
Preprint. Discussion started: 20 September 2023


Atmospheric Measurement Techniques Discussions

Sewage Overflow (CSO). These transects are quick crossings of closer, smaller plumes, (less than 20m from the source locations, around 150m in length, and 10-20 seconds transecting the plume) and are typical of the small enhancements in our previous urban observations (Ars et al., 2020).

3.1 Ashbridge's Bay Wastewater Treatment Plant

The Ashbridge's Bay Wastewater Treatment Plant is the largest sewage treatment facility in the GTA, processing the waste water of an estimated 1 733 500 people (The City of Toronto, 2022). The FLAME-GTA inventory reports that ABWWTP is the third largest single methane source in the City of Toronto, with an annual emission rate of 787 t $CH_4 yr^{-1}$ (Pak et al., 2021). The FLAME-GTA estimate is derived from the volume of biogas produced at ABWWTP, and accounts for biogas collection efficiency, and methane destruction efficiencies (Pak et al., 2021). In Canada's GHG reporting requirements, however, municipal wastewater treatment plants are not required to report methane emissions from the wastewater treatment process. The methane emissions reported to ECCC's GHG reporting program for ABWWTP (0.207 t CH_4 yr^{-1}) only include estimated fugitive emissions from the combustion of fossil gas brought into the WWTP (Environment and Climate Change Canada, 2021), and are not an estimate of methane emissions resulting from the biogas produced there.

From 2018, we have measured 44 downwind transects of methane plumes from ABWWTP on 21 different days using the UGGA bicycle laboratory, and 14 transects on 5 different days using the ECCC vehicle laboratory. These transects were conducted on public roads and bicycle paths. We revisited this site frequently to evaluate variability in emissions rates on various time scales, from seasonally to sub-hourly. Recently, Gålfalk et al. (2022) observed significant variability in CH_4 emissions on sub-hourly time scales following aerated and rest periods in WWTP infrastructure. To evaluate this possible variability, we conducted multiple transects over the course of a single day.

To estimate emissions from the ABWWTP, we first located the main emissions sources by summing the concentration-area of upwind concentration enhancements for each transect (Fig. 5a). We do this to locate grid cells which are repeatedly upwind of observed enhancements across a variety of wind directions. Here, we consider only wind direction and not wind speed for these calculations. We average observed in situ methane concentrations in 15m grid cells from each downwind transect. Then, we trace lines upwind of each grid cell, and add the average downwind measured concentration-area to the upwind grid cells. This approach failed to discriminate individual emissions sources, but it demonstrates that the majority of methane emissions we observed likely originate from the buildings located near the centre of the facility. The ponds and tanks also appear to be likely emissions sources.

For our Gaussian plume inversions, we use the fewest possible source locations to fit the major observed peaks from the transects with consistent observed winds, such that the wind direction did not change during the transect. We use the smallest number of modelled sources to avoid under-determined plume inversions. Based on our source modelling technique, we choose the buildings between First and Second Avenue as the location of the first point source (Fig. 5 b). The second source we include corresponds to the Eastern buildings and ponds. From fitting plumes advected by Westerly winds, measured along the Eastern bank of Ashbridge's Bay, we observed a persistent plume which required us to add a third source located at the Southern tanks. Similarly, when fitting plumes along Leslie St, the public road to the West of the facility under Easterly winds, we required a

https://doi.org/10.5194/amt-2023-193
Preprint. Discussion started: 20 September 2023

Atmospheric Measurement Techniques Discussions

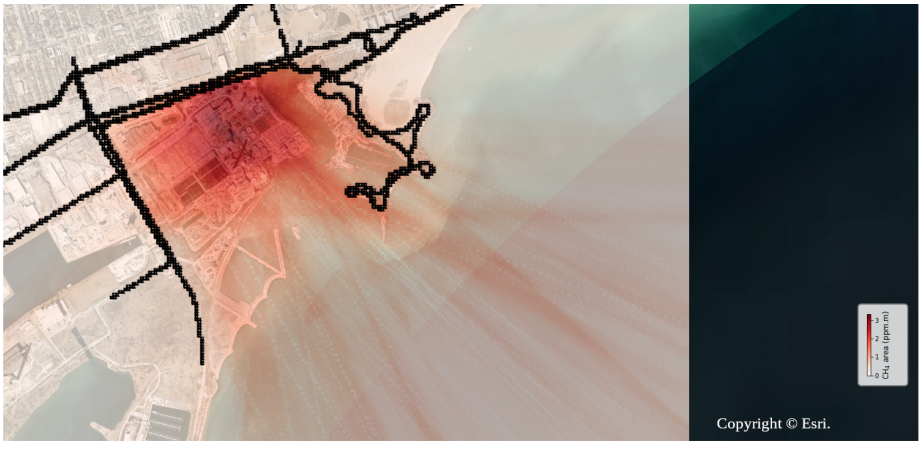

(a) From ESRI (2022).

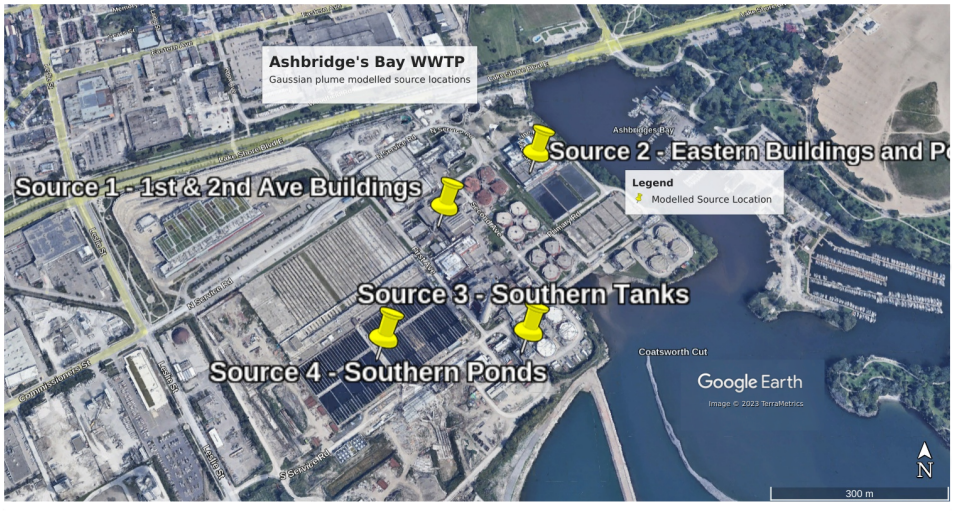

(b) From Google Earth (2023).

Figure 5. (a) Average concentrations in 15m grid cells from all transects are traced upwind. The heatmap is created from the sum of all of the upwind traces, with darker red indicating a higher total upwind concentration area, corresponding to likely emissions source locations. The black boxes represent the grid boxes sampled in the downwind transects. (b) ABWWTP source locations for the Gaussian plume inversion model.

fourth area source located at the Western ponds. All sources are labelled in Figure 5 b. The first three locations are modelled as point sources, since they are potential sites for leaks in biogas collection infrastructure. We modelled the fourth source as a circular area with a 20 m diameter, as this largest pond at the facility is likely to be a diffuse source. Further specifics of the inversion parameters are included in the Supplemental Information (S4.4).

https://doi.org/10.5194/amt-2023-193
Preprint. Discussion started: 20 September 2023

Atmospheric Measurement Techniques Discussions

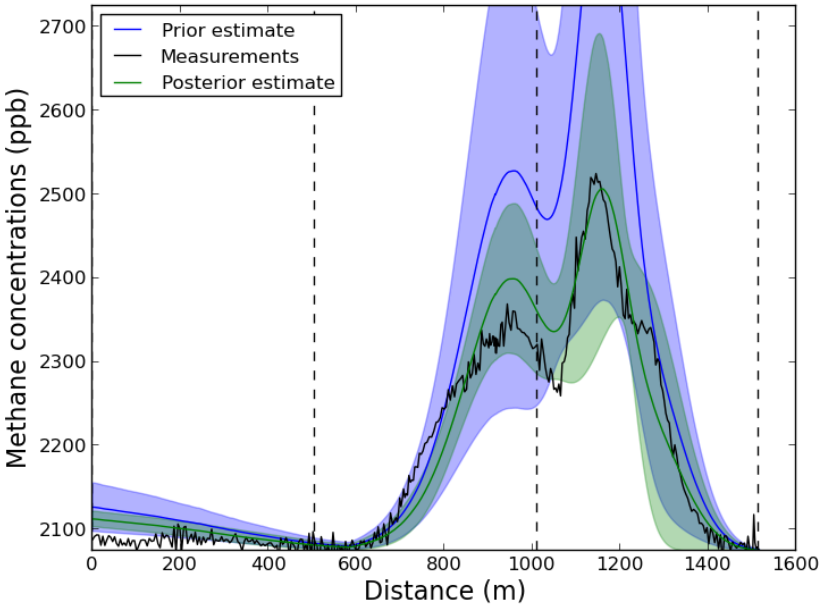

Figure 6. An optimized Gaussian plume model for the first transect recorded on 2020-08-31 using the UGGA bicycle laboratory. The transect was along Leslie Street, the major roadway West of ABWWTP, capturing methane plumes advected by Easterly winds.

Our prior emission rate comes from scaling the ABWWTP annual emissions reported in the FLAME-GTA inventory (Pak et al., 2021). When modelling the plumes, we found that prescribing 1/3 of the prior emissions to source 1, and the remaining emissions equally, with 2/9 for sources 2, 3, and 4 provided a good first estimate to fit observed data under a variety of wind directions. We used this distribution of emissions as the prior emissions for our inversions.

To estimate emissions based on our observed concentrations, we used a standard Gaussian plume area inversion. These large plume crossings are significantly less affected by the smoothing of the observed UGGA methane concentrations as plume transect time is several multiples of the mean residence time of the instrument. An example of an optimized Gaussian plume model is shown in Figure 6. A summary of all of our transects is presented in Figure 7. The mean emissions as measured by the UGGA bicycle platform were 1772 $\pm$ 815 kg day^{-1} (N=44), and 1613 $\pm$ 1156 kg day^{-1} (N=14) for the ECCC Picarro mobile laboratory. For the estimates from each mobile platform, the uncertainty is the standard deviation of all the estimated emissions. This corresponds to an annual emission rate of 647 $\pm$ 297 t yr^{-1} and 589 $\pm$ 422 t yr^{-1}, respectively. The greater uncertainty in the results from the vehicle laboratory are likely due to the smaller number of samples, and greater range in the time-of-year that these transects were conducted. A further analysis of temporal variability in the Supplemental Information (S4.2), but we find that a lack of winter observations prevents us from robustly determining if there is any seasonal variability. We note that the range of emissions estimates between the two laboratories are quite similar, with average emissions rates from each lab agreeing within uncertainty. We used rural stability classes, informed by public historic weather data from ECCC

https://doi.org/10.5194/amt-2023-193
Preprint. Discussion started: 20 September 2023

Atmospheric Measurement Techniques Discussions

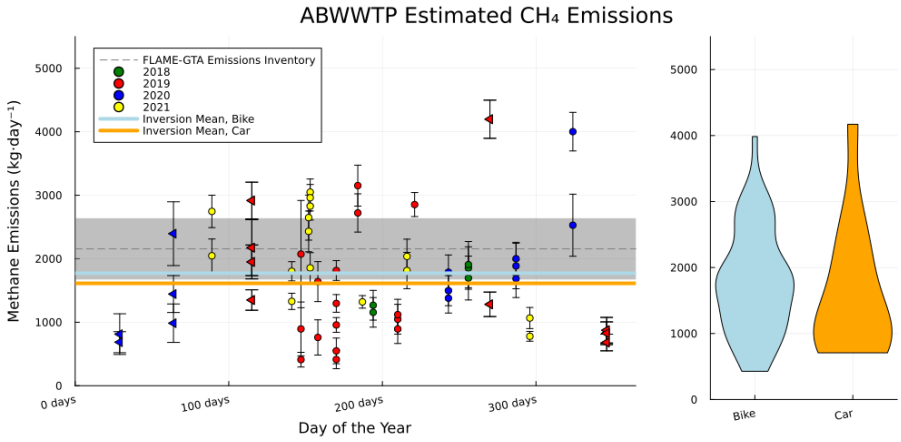

Figure 7. *Left:* Inversion results for all transects of ABWWTP. Bike data are shown with circle markers, and car data are triangles. The x axis denotes the number of days since the start of the calendar year. *Right:* Violin plots showing the relative distribution frequency of different estimated emissions rates from each mobile platform.

(Briggs, 1973). The inversion's sensitivity to the stability class, and other errors are discussed in the Supplemental Information (S4.3). Generally, the average inversion results are highly dependent on stability class, and we calculate a mean flux from the plant which is 70% greater when using urban stability classes. The average annual mean emissions calculated from the both laboratories agree within uncertainty with the FLAME-GTA inventory (787 ± 352 t yr^{-1}) (Pak et al., 2021).

3.2 Combined Sewage Overflow Containment Basins

The older downtown part of Toronto has a combined storm-water and wastewater sewage system for collecting and treating urban street rainwater runoff and sewage. Originally constructed in the 1990's as a storage and primary treatment facility to prevent combined sewage overflow (CSO) spillage into Lake Ontario, the Western Beaches Tunnel (WBT) system is an 85 000 m^3 wastewater storage facility designed to contain CSO during high rainfall events. The city recently addressed the operational issues with the Western Beaches Tunnel system, including removing sediment build-up in the system (The City of Toronto, 2020). The locations of the three major storage shafts are shown in Figure 8. On our bicycle surveys along Toronto's waterfront, we observe persistent methane plumes from the CSO ventilation grates near Lake Ontario in three locations: the Glendale Ave storage shaft, the Cowan Ave storage shaft, and the Strachen storage shaft and Battery Park pumping station.

Unlike the plumes observed from the ABWWTP, transects for the CSO basin plumes are shorter, and considerably nearer to the emission source (18-100m). As such, we find that to compute an accurate emission rate, we cannot rely on enhancement height measurements. We use normal Gaussian plume area inversions, which are equivalent to our smoothed plume area inversions. An example of a typical plume transect and fitted model is shown in Figure 9.

All CSO basin sources were modelled as a single ground-level point source. We chose the centroid of the ventilation grates as the source location at each site. The results of each inversion are shown in Figure 10. The mean daily estimate emission rates

https://doi.org/10.5194/amt-2023-193
Preprint. Discussion started: 20 September 2023

Atmospheric Measurement Techniques Discussions

Figure 8. The locations of the storage shafts in the Western Beaches Tunnel system. From Google Earth (2023).

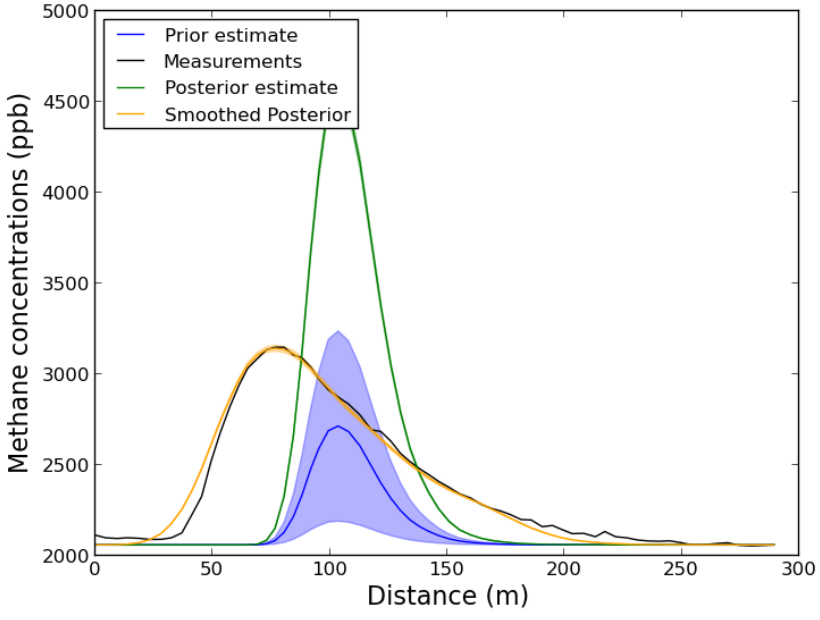

Figure 9. Measured and modelled CH_4 plumes from the Glendale storage shaft, from the 2021-08-11, 16:34 UTC transect. In this plot the prior emissions estimate is shown in blue, the normal Gaussian plume enhancement-area posterior is shown in green, and the smoothed Gaussian plume enhancement-area posterior is orange. Measured concentrations are shown in black.

https://doi.org/10.5194/amt-2023-193
Preprint. Discussion started: 20 September 2023

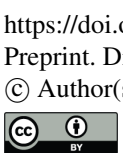

Atmospheric Measurement Techniques Discussions

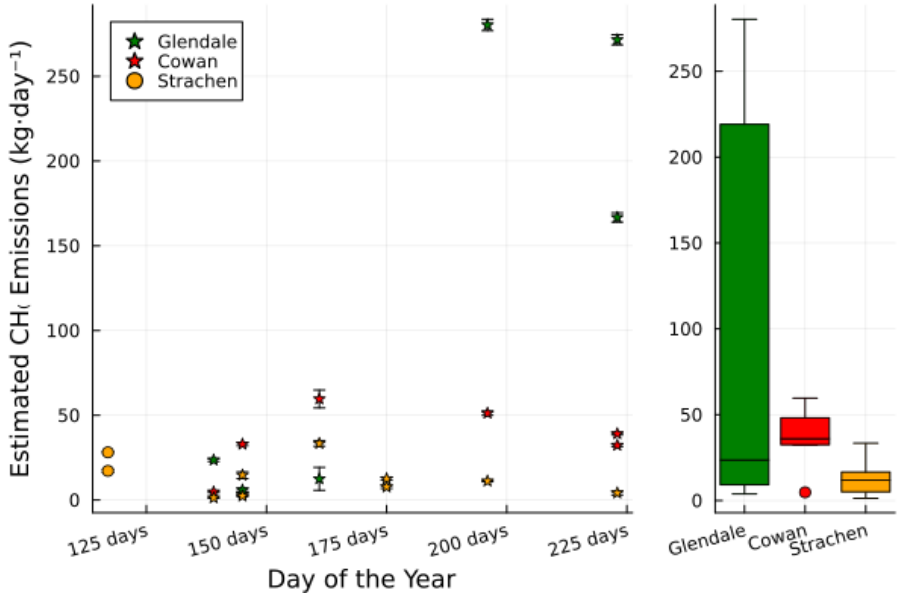

Figure 10. *Left:* Inversion results for all transects of the waterfront CSO basins, with stars denoting data from 2021, and circles denote data from 2022. The x axis denotes the number of days since the start of the calendar year. *Right:* box and whisker plots showing the range of estimated emission rates from the basins.

are 30.7, 12.3, and 108 kg/day for the Cowen, Strachen, and Glendale storage shafts, respectively. We expect the emissions from the CSOs to be highly heterogeneous and to change seasonally, with significant emissions only during summer (3 months of the year) due to increased precipitation and higher water temperatures. Therefore we would expect annual emissions to be around 14 t CH_4 yr^{-1}. These WBT emissions sources are not reported to the GHG reporting program, nor are they presently included in the FLAME-GTA inventory.

4 Discussion

Overall in this paper, we present an emissions estimation methodology, tested against a controlled release experiment designed to mimic observations of small sources commonly encountered in the urban environment. The CSO basins are a good example of the small sources we observe regularly during our mobile surveys. As with our controlled release experiment, the inversion results for the CSO basins are consistent between the unaltered Gaussian plume area inversions, and the smoothed plume area inversions. The smoothed enhancement height inversions, where we explicitly account for the instrument response function, also agree well with the estimates from the area inversions. The inversions using the unaltered Gaussian plume enhancement heights are biased low compared with the others. By taking into account the instrument flow-rate with our instrument response function, we are able to reconcile the differences between our peak concentration enhancement inversions, and Gaussian plume area inversions for the LGR UGGA. We did not test our emissions quantification methodology with a larger controlled release

https://doi.org/10.5194/amt-2023-193
Preprint. Discussion started: 20 September 2023


Atmospheric Measurement Techniques Discussions

experiment, because we were limited by the available resources for conducting such CH_4 releases. However, we use ABWWTP as a large source with reasonably well-estimated emissions in the FLAME-GTA inventory (Pak et al., 2021), to also test our Gaussian plume inversion methodology on a larger scale.

In recent literature, studies by Von Fischer et al. (2017) and Weller et al. (2019) use a log-log statistical model to estimate emissions based on the peak height of the observed concentration. This algorithm does not explicitly account for the distance to the emissions source, nor does it take into account other factors, such as atmospheric stability or wind speed, because those parameters were not measured as part of their initial mobile measurement campaign which consisted of geo-located observations with a Picarro G2301 (Von Fischer et al., 2017). The Weller et al. (2019) method has been used in a number of studies to estimate fossil gas distribution fugitive emissions rates from mobile survey data (Weller et al., 2020; Ars et al., 2020; Defratyka et al., 2021; Maazallahi et al., 2020). The meta-analysis of Vogel et al. (2023a), which analyzed data from mobile observations in several cities using the exact same approach shows that data from our bicycle UGGA laboratory are the most significant outlier, recording a greater percentage of "small" emissions sources than any of the other urban mobile methane measurement campaigns. This is likely due to two causes. The first is that our peak heights are reduced by our instrument response function. The second is that the survey routes of the bike tend to be constrained to the City of Toronto, along routes with suitable cycling infrastructure, potentially missing the larger fossil gas leaks near major roadways (Vogel et al., 2023a).

When we synthesize the results from our controlled release experiment and our survey data, we find that plume area is a more reliable and consistent proxy for emission rates than peak enhancement concentration (Figures 11 a and b). This corroborates previous work suggesting the peak area enhancements are a more consistent metric for estimating and quantifying emissions rates, as opposed to a statistical relationship based on peak enhancement heights (Ars et al., 2017, 2020). We consider inversions optimized with a Gaussian plume model area to be the best option for quantifying instantaneous emissions rates from mobile transect data.

In Figure 12, we compare our estimated emissions rates using four different Gaussian plume inversions, and the statistical model for the CSO basin and controlled release experiment transects. There is excellent agreement between the enhancement area and the smoothed enhancement area optimizations. This is expected, as the smoothing operation conserves the observed total concentration enhancement area from the transect. There is a significant correlation between the area inversions and the smoothed enhancement height inversion for the small source bicycle transects. This suggests that accounting for the instrument response function for the LGR UGGA is necessary to correct the Gaussian plume enhancement height model for short, near-to-source transects. The normal Gaussian enhancement height inversion is biased low compared to the other methods, reflecting the impact of the asymmetrical smoothing of the lower flow-rate UGGA. The statistical relation from (Weller et al., 2019) is the most negatively biased with respect to the other results. Thus, we caution against the use of this statistical algorithm for quantifying individual sources, especially in cases where the gas concentration observations are affected by the response function of the gas analyzer.

We further demonstrate the comparability of the enhancement area as an emissions quantification metric by examining the normalized cumulative emissions relative to normalized emitter size for three different emissions metrics: the measured enhancement area, the measured enhancement height, and the Weller et al. (2019) statistical algorithm for the UGGA bicycle

https://doi.org/10.5194/amt-2023-193
Preprint. Discussion started: 20 September 2023

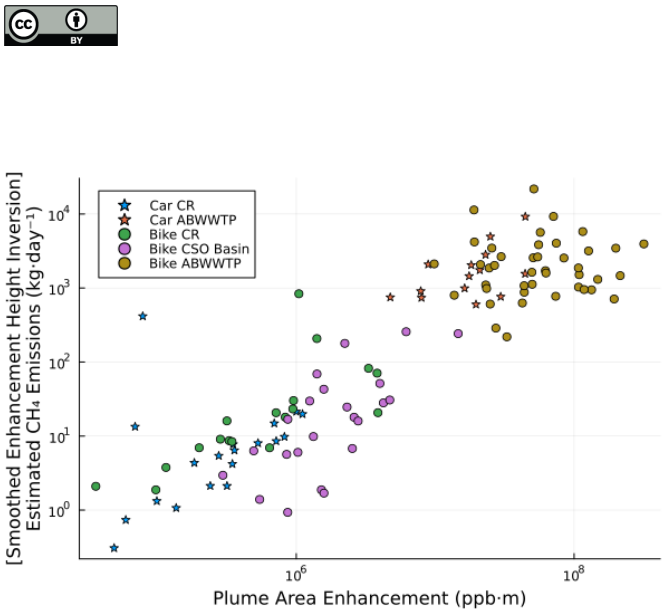

(a) The smoothed enhancement height inversion results vs. the measured plume area.

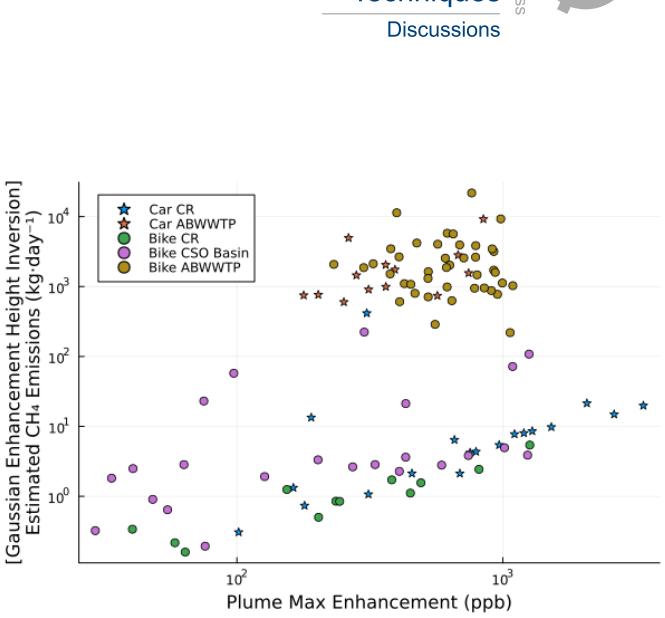

(b) The Gaussian enhancement height inversion results vs. the measured enhancement height.

Figure 11. (a) Demonstrates that inversion results that are independent of the plume area—but which account for instrument response—are better correlated with the measured plume area than the measured peak enhancement heights, shown in (b). In (b) one inversion from the car ABWWTP dataset is omitted, and two inversions from the bike ABWWTP dataset are omitted for non-physical negative inversion optimizations. Note the logarithmic scales on both axes of the two plots.

laboratory and the ECCC Picarro vehicle laboratory for the plumes quantified in this study. We demonstrate in Figure 13 that the most consistent emissions metrics between the two mobile laboratories is the enhancement area. In Vogel et al. (2023a), which uses the Weller et al. (2019) algorithm to compare mobile observations across 12 different cities, the normalized cumulative emissions trend from our bicycle laboratory is an outlier from the rest of the mobile CH_4 measurement laboratories, with the first 17^{th} percent of emitters measured were deemed responsible for 50% of observed emissions. For the other laboratories in that study, the first 8^{th} percent or fewer sources were responsible for 50% of the observed cumulative emissions. In addition to the reasons stated in that publication for the differences between our bicycle laboratory and the others, this difference is also likely to be a consequence of the unsuitability of the Weller et al. (2019) methodology for the LGR UGGA instrument, due to the lower enhancements recorded as a result of the instrument response function. In Figure 13, we compute the cumulative emissions as a function of the ranked emission sources (ranked from highest emissions to lowest emissions). The cumulative emissions are computed for the bicycle and vehicle data when evaluating emissions using the peak area and enhancement height, and also using the Weller et al. (2019) method. Figure 13 demonstrates that the most significant differences between emissions metrics are between estimates using the Weller et al. (2019) technique.

https://doi.org/10.5194/amt-2023-193
Preprint. Discussion started: 20 September 2023

Atmospheric Measurement Techniques Discussions

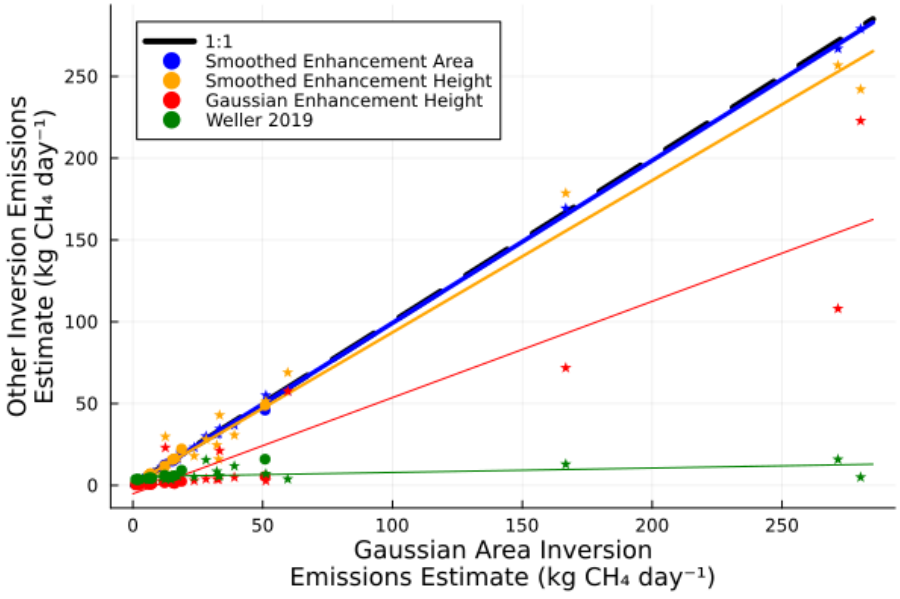

Figure 12. Correlation plot comparing the results of various emission estimate calculations on the CSO (stars) and controlled release transects (circles) relative to the uncorrected Gaussian plume area inversion. Lines of best fit for each inversion, relative to the Gaussian Plume area inversion are shown.

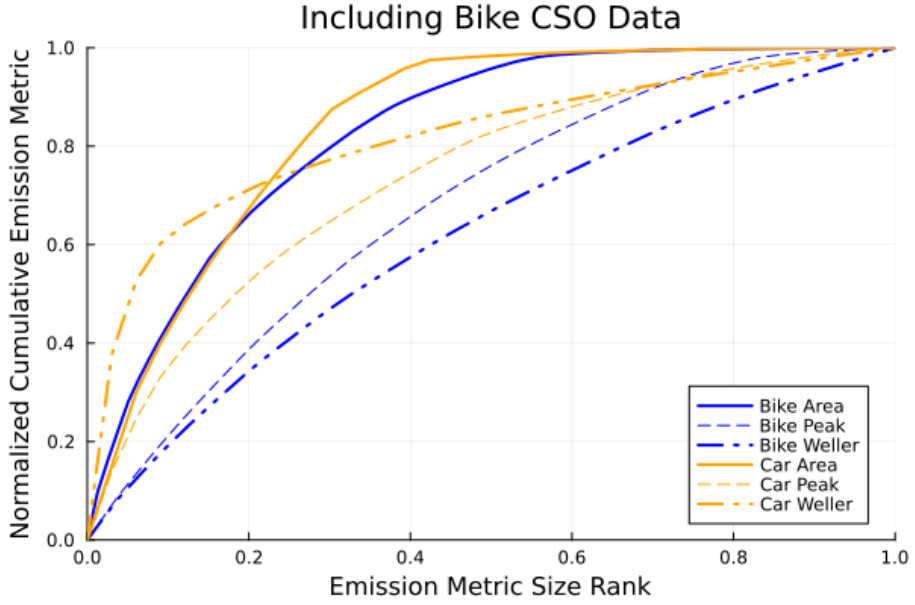

Figure 13. Normalized cumulative emissions relative to normalized emitter size ranked from high to low for three emissions metrics.

https://doi.org/10.5194/amt-2023-193
Preprint. Discussion started: 20 September 2023


Atmospheric Measurement Techniques Discussions

5 Conclusions

In this work, we demonstrate the importance and applicability of accounting for the instrument response function when using Gaussian plume inversions to quantify emissions from mobile in situ observations. In the case of the low flow-rate LGR UGGA, convolution by an asymmetric smoothing window greatly improves the agreement between observed and modelled Gaussian plume enhancements, as well as minimizing differences between coincidental observations with other GHG analyzers. For estimating emissions rates, we find that the Gaussian enhancement area inversion is sufficient for both mobile laboratories and is robust to flow-rate issues, as long as the entire plume is sampled. Like previous studies, we demonstrate that the plume enhancement area provides a more consistent observation metric between different experimental setups. Furthermore, we demonstrate that enhancement area inversions and smoothed Gaussian plumes are practically equal to one another. We also demonstrate how approximate sources can be inferred using concentration vector triangulation techniques from downwind measurements.

We utilize the Gaussian enhancement area inversion technique to quantify emissions from the largest WWTP in the City of Toronto. From this analysis, we can demonstrate that the FLAME-GTA inventory estimate for CH_4 emissions from ABWWTP is consistent with our estimates from our mobile plume optimizations. In Canada's GHG reporting program, CH_4 emissions from municipal wastewater treatment plants are not required to be reported. Considering the relative CO_{2eq} of the methane emissions we estimate from our mobile observations, we argue that such emissions should be included in the GHG reporting requirements. For facilities that capture and utilize the biogas produced, we suggest that estimates derived from the volume of gas produced, like the estimates in the FLAME-GTA inventory, are a reasonable first guess of the facility's methane emissions for municipal WWTP's. The relevant formula is presented again in the Supplemental Information (S4.2). Since the FLAME-GTA inventory emissions estimates for ABWWTP agree within error of our emissions estimates from both of our mobile laboratories, we do not suggest an update to the FLAME-GTA inventory for this facility, but we do suggest adding the Western Beaches Tunnel system emissions to the FLAME-GTA inventory. If we take our inversion results to represent the facility's average emissions, the system could represent a combined source over 55 $t{\cdot}yr^{-1}$. However, this is likely an overestimate, as we expect some seasonality in the emissions pattern due to temperature. We recommend additional targeted measurements at the CSO basins throughout the year to determine if the completed construction work has influenced methane emissions from the system.

Importantly, this study also demonstrates how mobile observations from different experimental platforms can be readily compared against one another by accounting for the residence time distribution of analyzers with slower flow-rates and longer mean residence times, such as the LGR UGGA. In future studies, the instrument response function could be more rigorously evaluated for different experimental setups. We suggest that the response function could be determined by a deconvolution of the observed gas concentrations, subjected to a known concentration perturbation, such as a rectangular pulse created with timed electronic valves. This would allow researchers to rigorously evaluate differences between different gas analyzers used for mobile measurement studies. Short of such analysis, we find that using enhancement areas is a suitable technique for comparing observations between different gas analyzers and mobile platforms.

https://doi.org/10.5194/amt-2023-193
Preprint. Discussion started: 20 September 2023


Atmospheric Measurement Techniques Discussions

Overall, in this study we demonstrate that estimating small emission rates with Bayesian optimization of Gaussian enhancement areas for transects close to the source is a useful tool for constraining the magnitude of methane emissions from mobile in situ GHG concentration data. Our controlled release experiment demonstrated that repeated measurements are essential for constraining the source emission rate, and that estimated instantaneous emission rates can vary widely between sequential plume transects. We conclude that Gaussian plume inversions are a useful tool to quantify emissions from mobile in situ CH_4 measurements, and that inversions should be calculated either using the plume area, or with explicit modelling of the instrument response function for inversions using the enhancement height. We demonstrate that estimating emissions using concentration enhancement areas is a more robust and comparable method of estimating emissions between various mobile laboratories. We recognize that additional work is needed to collect and analyze controlled release experiments from other platforms and groups globally. This work to develop standard methodologies for use by academic, non-governmental organizations, and private sector providers will allow for a more straightforward comparison between emissions estimates from different groups.

Data availability. Data from the bicycle lab are openly available from the on the University of Toronto achieve (Wunch et al., 2018; Ars et al., 2019; Gillespie et al., 2022a, b, 2023). The ECCC vehicle data are available from a web achieve (Vogel et al., 2023b).

Author contributions. DW, SA, FV, and LG formulated the research aim for this study. DW and SA assisted with data curation. LG completed the formal analysis for this study. DW and FV acquired the funding for this study. LG, SA, JW, LK, TF, MR, MK, AM, and SG completed the research investigation. SA and LG devised the research methodology. DW, FV, and MK supervised and guided the experimental work, provided resources for the project, and administered the research project. LG and SA and worked on the software and data visualization for this publication. LG prepared the manuscript with contributions from all of the co-authors. All authors contributed to the review and editing of the study.

Competing interests. The authors declare that they have no conflict of interest.

Acknowledgements. Funding for this work was provided by the Natural Sciences and Engineering Research Council of Canada grants RGPIN-2021-03525 and RGPAS-2021-00024, the Canadian Foundation for Innovation grant no. 35278, and Ontario Research Fund project grant RI-35278.

The authors acknowledge the senior engineers at Toronto Water for clarifying and communicating about municipal wastewater treatment reporting requirements. The authors also thank the team of undergraduate assistants, including Cameron MacDonald, Rica Cruz, Juliette Lavoie, Colin Arrowsmith, Sajjan Heerah, and Emily Knuckey for their contributions to the UofT GHG measurement campaigns.

https://doi.org/10.5194/amt-2023-193
Preprint. Discussion started: 20 September 2023

Atmospheric Measurement Techniques Discussions

References

Ars, S., Broquet, G., Kwok, C. Y., Roustan, Y., Wu, L., Arzoumanian, E., and Bousquet, P.: Statistical atmospheric inversion of local gas emissions by coupling the tracer release technique and local-scale transport modelling: A test case with controlled methane emissions, Atmospheric Measurement Techniques, 10, 5017–5037, https://doi.org/10.5194/amt-10-5017-2017, 2017.

Ars, S., Lavoie, J., Cruz, R., Macdonald, C., Beauregard, G., Cunningham, L., and Wunch, D.: GTA Bike Surveys - Summer 2019 - Uncalibrated data, https://doi.org/10.5683/SP2/SBIZ1F, 2019.

Ars, S., Vogel, F., Arrowsmith, C., Heerah, S., Knuckey, E., Lavoie, J., Lee, C., Pak, N. M., Phillips, J. L., and Wunch, D.: Investigation of the spatial distribution of methane sources in the greater Toronto area using mobile gas monitoring systems, Environmental Science and Technology, 54, 15 671–15 679, https://doi.org/10.1021/acs.est.0c05386, 2020.

Atherton, E., Risk, D., Fougère, C., Lavoie, M., Marshall, A., Werring, J., Williams, J. P., and Minions, C.: Mobile measurement of methane emissions from natural gas developments in northeastern British Columbia, Canada, Atmospheric Chemistry and Physics, 17, 12 405–12 420, https://doi.org/10.5194/acp-17-12405-2017, 2017.

Bailey, D., Brode, R., Bennett, E., Dicke, J., Eskridge, R., Garrison, M., Irwin, J., Koerber, M., Lockhart, T., Method, T., Perkins, S., Wilson, R., and Cannady, B.: Meteorological Monitoring Guidance for Regulatory Modeling Applications, Tech. Rep. EPA-454/R-99-005, US EPA, Research Triangle Park, https://www.epa.gov/sites/default/files/2020-10/documents/mmgrma_0.pdf, 2000.

Baillie, J., Risk, D., Atherton, E., O'connell, E., Fougère, C., Bourlon, E., and Mackay, K.: Methane emissions from conventional and unconventional oil and gas production sites in southeastern Saskatchewan, Canada, Environmental Research Communications, 1, https://doi.org/10.1088/2515-7620/ab01f2, publisher: IOP Publishing, 2019.

Brantley, H. L., Thoma, E. D., Squier, W. C., Guven, B. B., and Lyon, D.: Assessment of methane emissions from oil and gas production pads using mobile measurements, Environmental Science and Technology, 48, 14 508–14 515, https://doi.org/10.1021/es503070q, 2014.

Briggs, G. A.: Diffusion estimation for small emissions. Preliminary report, Tech. rep., Air Resources Atmospheric Turbulence and Diffusion Laboratory, NOAA, Oak Ridge, Tennessee, http://www.osti.gov/scitech//servlets/purl/5118833-byrnco/, iSBN: TID-28289 United States10.2172/5118833Wed Feb 06 16:52:02 EST 2008Dep. NTIS, PC A04/MF A01.TIC; EDB-78-070484English, 1973.

Chen, J., Dietrich, F., Maazallahi, H., Forstmaier, A., Winkler, D., Hofmann, M. E. G., Denier van der Gon, H., and Röckmann, T.: Methane emissions from the Munich Oktoberfest, Atmospheric Chemistry and Physics, 20, 3683–3696, https://doi.org/10.5194/acp-20-3683-2020, 2020.

Crippa, M., Guizzardi, D., Banja, M., Solazzo, E., Muntean, M., Schaaf, E., Pagani, F., Monforti-Ferrario, F., Olivier, J.G.J., Quadrelli, R., Risquez Martin, A., Taghavi-Moharamli, P., Grassi, G., Rossi, S., Oom, D.,, Branco, A., San-Miguel, J., and Vignati, E.: CO2 emissions of all world countries: JRC/IEA/PBL 2022 report., Publications Office, LU, https://data.europa.eu/doi/10.2760/730164, 2022.

Defratyka, S. M., Paris, J. D., Yver-Kwok, C., Fernandez, J. M., Korben, P., and Bousquet, P.: Mapping Urban Methane Sources in Paris, France, Environmental Science and Technology, 55, 8583–8591, https://doi.org/10.1021/acs.est.1c00859, 2021.

Delre, A., Hensen, A., Velzeboer, I., van den Bulk, P., Edjabou, M. E., and Scheutz, C.: Methane and ethane emission quantifications from onshore oil and gas sites in Romania, using a tracer gas dispersion method, Elementa: Science of the Anthropocene, 10, 000 111, https://doi.org/10.1525/elementa.2021.000111, 2022.

Environment and Climate Change Canada: Facility Greenhouse Gas (GHG) Data, https://data-donnees.ec.gc.ca/data/substances/monitor/greenhouse-gas-reporting-program-ghgrp-facility-greenhouse-gas-ghg-data/PDGES-GHGRP-GHGEmissionsGES-2004-Present.csv, 2021.

Fernandez, J., Maazallahi, H., France, J., Menoud, M., Corbu, M., Ardelean, M., Calcan, A., Townsend-Small, A., van der Veen, C., Fisher, R., Lowry, D., Nisbet, E., and Röckmann, T.: Street-level methane emissions of Bucharest, Romania and the dominance of urban wastewater., Atmospheric Environment: X, 13, 100 153, https://doi.org/10.1016/j.aeaoa.2022.100153, 2022.

Gillespie, L., Ars, S., Feng, C., Mostafavi Pak, N., and Wunch, D.: GTA Bike Surveys - Summer 2020 - Calibrated data, https://doi.org/10.5683/SP3/JEIZIF, 2022a.

Gillespie, L., Ars, S., Raczkowski, M., Mostafavi Pak, N., and Wunch, D.: GTA Bike Surveys - Summer 2021 - Calibrated data, https://doi.org/10.5683/SP3/ZGMAI7, 2022b.

Gillespie, L., Ars, S., Kandapath, M., Gu, S., Mann, A., Mostafavi Pak, N., and Wunch, D.: GTA Bike Surveys - Summer 2022 - Calibrated data, https://doi.org/10.5683/SP3/PGAIV7, 2023.

Gålfalk, M., Påledal, S. N., Sehlén, R., and Bastviken, D.: Ground-based remote sensing of CH4 and N2O fluxes from a wastewater treatment plant and nearby biogas production with discoveries of unexpected sources, Environmental Research, 204, 111 978, https://doi.org/10.1016/j.envres.2021.111978, 2022.

Herrero Ortega, S., Romero González-Quijano, C., Casper, P., Singer, G. A., and Gessner, M. O.: Methane emissions from contrasting urban freshwaters: Rates, drivers, and a whole-city footprint, Global Change Biology, 25, 4234–4243, https://doi.org/10.1111/gcb.14799, 2019.

Hugenholtz, C. H., Vollrath, C., Gough, T., Wearmouth, C., Fox, T., Barchyn, T., and Billinghurst, C.: Methane emissions from above-ground natural gas distribution facilities in the urban environment: A fence line methodology and case study in Calgary, Alberta, Canada, Journal of the Air & Waste Management Association, 71, 1319–1332, https://doi.org/10.1080/10962247.2021.1942316, 2021.

IPCC: Climate Change 2013: The Physical Science Basis. Contribution of Working Group I to the Fifth Assessment Report of the Intergovernmental Panel on Climate Change, Cambridge University Press, Cambridge, United Kingdom, https://doi.org/10.1017/CBO9781107415324.Summary, 2013.

Kirschbaum, M. U.: Climate-change impact potentials as an alternative to global warming potentials, Environmental Research Letters, 9, https://doi.org/10.1088/1748-9326/9/3/034014, 2014.

Kumar, P., Broquet, G., Caldow, C., Laurent, O., Gichuki, S., Cropley, F., Yver-Kwok, C., Fontanier, B., Lauvaux, T., Ramonet, M., Shah, A., Berthe, G., Martin, F., Duclaux, O., Juery, C., Bouchet, C., Pitt, J., and Ciais, P.: Near-field atmospheric inversions for the localization and quantification of controlled methane releases using stationary and mobile measurements, Quarterly Journal of the Royal Meteorological Society, pp. 1886–1912, https://doi.org/10.1002/qj.4283, 2022.

Lamb, B. K., Mcmanus, J. B., Shorter, J. H., Kolb, C. E., Mosher, B., Harriss, R. C., Allwine, E., Blaha, D., Howard, T., Guenther, A., Lott, R. A., Siverson, R., Westberg, H., and Zimmerman, P.: Development of Atmospheric Tracer Methods To Measure Methane Emissions from Natural Gas Facilities and Urban Areas, Environmental Science and Technology, 29, 1468–1479, https://doi.org/10.1021/es00006a007, 1995.

Lamb, B. K., Edburg, S. L., Ferrara, T. W., Howard, T., Harrison, M. R., Kolb, C. E., Townsend-Small, A., Dyck, W., Possolo, A., and Whetstone, J. R.: Direct measurements show decreasing methane emissions from natural gas local distribution systems in the United States, Environmental Science and Technology, 49, 5161–5169, https://doi.org/10.1021/es505116p, 2015.

Lamb, B. K., Cambaliza, M. O., Davis, K. J., Edburg, S. L., Ferrara, T. W., Floerchinger, C., Heimburger, A. M., Herndon, S., Lauvaux, T., Lavoie, T., Lyon, D. R., Miles, N., Prasad, K. R., Richardson, S., Roscioli, J. R., Salmon, O. E., Shepson, P. B., Stirm, B. H., and Whetstone, J.: Direct and Indirect Measurements and Modeling of Methane Emissions in Indianapolis, Indiana, Environmental Science and Technology, 50, 8910–8917, https://doi.org/10.1021/acs.est.6b01198, 2016.

https://doi.org/10.5194/amt-2023-193
Preprint. Discussion started: 20 September 2023

Atmospheric Measurement Techniques Discussions

Lebel, E. D., Lu, H. S., Vielstädte, L., Kang, M., Banner, P., Fischer, M. L., and Jackson, R. B.: Methane Emissions from Abandoned Oil and Gas Wells in California, Environmental Science & Technology, 54, 14 617–14 626, https://doi.org/10.1021/acs.est.0c05279, 2020.

Lebel, E. D., Finnegan, C. J., Ouyang, Z., and Jackson, R. B.: Methane and NO $_x$ Emissions from Natural Gas Stoves, Cooktops, and Ovens in Residential Homes, Environmental Science & Technology, 56, 2529–2539, https://doi.org/10.1021/acs.est.1c04707, 2022.

Maazallahi, H., Fernandez, J. M., Menoud, M., Zavala-Araiza, D., Weller, Z. D., Schwietzke, S., Von Fischer, J. C., Denier Van Der Gon, H., and Röckmann, T.: Methane mapping, emission quantification, and attribution in two European cities: Utrecht (NL) and Hamburg (DE), Atmospheric Chemistry and Physics, 20, 14 717–14 740, https://doi.org/10.5194/acp-20-14717-2020, 2020.

MacKay, K., Lavoie, M., Bourlon, E., Atherton, E., O'Connell, E., Baillie, J., Fougère, C., and Risk, D.: Methane emissions from upstream oil and gas production in Canada are underestimated, Scientific Reports, 11, 11:8041, https://doi.org/10.1038/s41598-021-87610-3, publisher: Nature Publishing Group UK ISBN: 4159802187610, 2021.

Mallet, V., Quélo, D., Sportisse, B., de Biasi, M. A., Debry, \., Korsakissok, I., Wu, L., Roustan, Y., Sartelet, K., Tombette, M., and Foudhil, H.: Technical note: The air quality modeling system polyphemus, Atmospheric Chemistry and Physics, 7, 5479–5487, https://doi.org/10.5194/acp-7-5479-2007, 2007.

Mitchell, A.: A comparison of short-term dispersion estimates resulting from various atmospheric stability classification methods, Atmospheric Environment, 16, 765–773, https://doi.org/10.1016/0004-6981(82)90394-8, 1982.

Moore, D. P., Li, N. P., Wendt, L. P., Castañeda, S. R., Falinski, M. M., Zhu, J.-J., Song, C., Ren, Z. J., and Zondlo, M. A.: Underestimation of Sector-Wide Methane Emissions from United States Wastewater Treatment, Environmental Science & Technology, 57, 4082–4090, https://doi.org/10.1021/acs.est.2c05373, 2023.

Mønster, J., Samuelsson, J., Kjeldsen, P., and Scheutz, C.: Quantification of methane emissions from 15 Danish landfills using the mobile tracer dispersion method, Waste Management, 35, 177–186, https://doi.org/10.1016/j.wasman.2014.09.006, 2015.

O'Connell, E., Risk, D., Atherton, E., Bourlon, E., Fougère, C., Baillie, J., Lowry, D., and Johnson, J.: Methane emissions from contrasting production regions within Alberta, Canada: Implications under incoming federal methane regulations, Elementa, 7, 1–13, https://doi.org/10.1525/elementa.341, 2019.

Pak, N. M., Heerah, S., Zhang, J., Chan, E., Worthy, D., Vogel, F., and Wunch, D.: The Facility Level and Area Methane Emissions inventory for the Greater Toronto Area (FLAME-GTA), Atmospheric Environment, 252, 118 319, https://doi.org/10.1016/j.atmosenv.2021.118319, publisher: Elsevier Ltd, 2021.

Rella, C. W., Tsai, T. R., Botkin, C. G., Crosson, E. R., and Steele, D.: Measuring Emissions from Oil and Natural Gas Well Pads Using the Mobile Flux Plane Technique, Environmental Science & Technology, 49, 4742–4748, https://doi.org/10.1021/acs.est.5b00099, 2015.

Shorter, J. H., McManus, J. B., Kolb, C. E., Allwine, E. J., Lamb, B. K., Mosher, B. W., Harriss, R. C., Partchatka, U., Fischer, H., Harris, G. W., Crutzen, P. J., and Karbach, H. J.: Methane emission measurements in urban areas in Eastern Germany, Journal of Atmospheric Chemistry, 24, 121–140, https://doi.org/10.1007/BF00162407, 1996.

Takriti, M., Wynn, P. M., Elias, D. M., Ward, S. E., Oakley, S., and McNamara, N. P.: Mobile methane measurements: Effects of instrument specifications on data interpretation, reproducibility, and isotopic precision, Atmospheric Environment, 246, 118 067, https://doi.org/10.1016/j.atmosenv.2020.118067, publisher: Elsevier Ltd, 2021.

Tavakkoli, S., Feng, L., Miller, S. M., and Jordaan, S. M.: Implications of Generation Efficiencies and Supply Chain Leaks for the Life Cycle Greenhouse Gas Emissions of Natural Gas-Fired Electricity in the United States, Environmental Science & Technology, 56, 2540–2550, https://doi.org/10.1021/acs.est.1c05246, 2022.

https://doi.org/10.5194/amt-2023-193
Preprint. Discussion started: 20 September 2023

Atmospheric Measurement Techniques Discussions

The City of Toronto: Amendment to Purchase Order No. 6048827 for the Western Beaches Tunnel-Sewer Chamber Modifications and Other Alterations Project and Amendment to Purchase Order No. 6046087 for Contract Administration Services, Tech. rep., The City of Toronto, Toronto, http://app.toronto.ca/tmmis/viewAgendaItemHistory.do?item=2014.BD208.1, 2020.

The City of Toronto: TransformTO Net Zero Strategy: A climate action pathway to 2030 and beyond, Tech. rep., The City of Toronto, https://www.toronto.ca/legdocs/mmis/2021/ie/bgrd/backgroundfile-173758.pdf, 2021.

The City of Toronto: Ashbridge's Bay Wastewater treatment Plant 2021 Annual Report, Tech. rep., Toronto, 2022.

Thoma, E. and DeWees, J.: OTM 33 Geospatial Measurement of Air Pollution, Remote Emissions Quantification (GMAP-REQ) and OTM33A Geospatial Measurement of Air Pollution-Remote Emissions Quantification-Direct Assessment (GMAP-REQ-DA), Tech. rep., US EPA, 2014.

Turnbull, J. C., DeCola, P., Mueller, K., Vogel, F., Agusti-Panareda, A., Ahn, D., Baidar, S., Bovensmann, H., Brewer, A., Brunner, D., Chen, H., Chen, J., Chevallier, F., Crisp, D., Christen, A., Cohen, R., Davis, K. J., Dietrich, F., Engelen, R., Feigenwinter, C., Fix, A., Gioli, B., Gurney, K., Hajny, K., Hakkarainen, J., Hammer, S., Hase, F., Hilton, T. W., Hutyra, L., Järvi, L., Jeong, S., Karion, A., Kim, J., Lauvaux, T., Lin, J., Loh, Z., Lopez-Coto, I., Matthews, B., Miles, N., Mitchell, L., Murray, L., Nehrkorn, T., Pak, N. M., Papale, D., Park, H., Pisso, I., Pitt, J., Ramonet, M., Rayner, P., Röckman, T., Roiger, A., Shepson, P., Sperlich, P., Velasco, E., Vermuelen, A., Vimont, I., Vogt, R., Whetstone, J. R., Winbourne, J., and Xueref-Remy, I.: IG3IS Urban Greenhouse Gas Emission Observation and Monitoring Good Research Practice Guidelines, GAW Report No. 275, WMO, GAW, IG3IS, https://library.wmo.int/index.php?lvl=notice_display&id=22120, 2022.

Vogel, F., Ars, A., Wunch, D., J Lavoie, Maazallahi, H, T Röckmann, J Necki, J Bartyzel, P Jagoda, D Lowry, J France, J Fernandez, S Bakkaloglu, R Fisher, M Lanoiselle, H Chen, M Oudshoorn, C Yver-Kwok, S Defratyka, J.A Morgui, C Estruch, R Curcoll, C Grossi, J Chen, F Dietrich, A Forstmaier, Denier van der Gon, H., S.N.C Dellaert, J Salo, M Corbu, S.S Iancu, A.S. Tudor, A.I Scarlat, and A Calcan: Ground-based mobile measurements to track urban methane emissions from natural gas in twelve cities across eight countries, Some Journal (in review), 2023a.

Vogel, F., Ars, S., and Gillespie, L.: GTA Vehicle Surveys of Ashbridges Bay Wastewater Treatment Plant, https://crd-data-donnes-rdc.ec.gc.ca/CCMR/publications/GTA_Car_Surveys_Gillespie_2023, 2023b.

Vogt, J., Laforest, J., Argento, M., Kennedy, S., Bourlon, E., Lavoie, M., and Risk, D.: Active and inactive oil and gas sites contribute to methane emissions in western Saskatchewan, Canada, Elementa, 10, 1–14, 2022.

Von Fischer, J. C., Cooley, D., Chamberlain, S., Gaylord, A., Griebenow, C. J., Hamburg, S. P., Salo, J., Schumacher, R., Theobald, D., and Ham, J.: Rapid, Vehicle-Based Identification of Location and Magnitude of Urban Natural Gas Pipeline Leaks, Environmental Science and Technology, 51, 4091–4099, https://doi.org/10.1021/acs.est.6b06095, 2017.

Wang, Y., Tang, J., Li, F., Xie, D., Zuo, F., Yu, X., Xu, Y., and Chen, J.: Measurement of methane emissions from CNG fueling stations in East China, Environmental Science and Pollution Research, https://doi.org/10.1007/s11356-022-20929-0, publisher: Springer Berlin Heidelberg ISBN: 1135602220, 2022.

Weller, Z. D., Yang, D. K., and Von Fischer, J. C.: An open source algorithm to detect natural gas leaks from mobile methane survey data, PLoS ONE, 14, 1–18, https://doi.org/10.1371/journal.pone.0212287, iSBN: 1111111111, 2019.

Weller, Z. D., Hamburg, S. P., and Von Fischer, J. C.: A National Estimate of Methane Leakage from Pipeline Mains in Natural Gas Local Distribution Systems, Environmental Science and Technology, 54, 8958–8967, https://doi.org/10.1021/acs.est.0c00437, 2020.

https://doi.org/10.5194/amt-2023-193
Preprint. Discussion started: 20 September 2023

Wielgosz, R., Forgan, B., Del Campo Maldonado, D., Rea, A., Woolliams, E., Fulford, J., Madonna, F., Whetstone, J., DeCola, P., Vermeulen, A., Flores, E., and Ruedi, I.: Metrology for Climate Action, IOM Report, Rapport BIPM-2023/03 142, WMO, BIPM, https://doi.org/10.59161/Rapport202303, 2023.

Williams, J. P., Ars, S., Vogel, F., Regehr, A., and Kang, M.: Differentiating and Mitigating Methane Emissions from Fugitive Leaks from Natural Gas Distribution, Historic Landfills, and Manholes in Montréal, Canada, Environmental Science & Technology, 56, 16 686–16 694, https://doi.org/10.1021/acs.est.2c06254, 2022.

Wunch, D., Arrowsmith, C., Ars, S., Knuckey, E., Mostafavi Pak, N., and Phillips, J. L.: GTA Bike Surveys - Summer 2018 - Calibrated data, https://doi.org/10.5683/SP2/U5CVFZ, 2018.

Yacovitch, T. I., Herndon, S. C., Pétron, G., Kofler, J., Lyon, D., Zahniser, M. S., and Kolb, C. E.: Mobile Laboratory Observations of Methane Emissions in the Barnett Shale Region, Environmental Science and Technology, 49, 7889–7895, https://doi.org/10.1021/es506352j, 2015.

Yacovitch, T. I., Neininger, B., Herndon, S. C., Van Der Gon, H. D., Jonkers, S., Hulskotte, J., Roscioli, J. R., and Zavala-Araiza, D.: Methane emissions in the Netherlands: The Groningen field, Elementa, 6, https://doi.org/10.1525/elementa.308, 2018.

Zavala-Araiza, D., Herndon, S. C., Roscioli, J. R., Yacovitch, T. I., Johnson, M. R., Tyner, D. R., Omara, M., and Knighton, B.: Methane emissions from oil and gas production sites in Alberta, Canada, Elementa, 6, https://doi.org/10.1525/elementa.284, 2018.